doi: 10.18720/MCE.82.8

Natural oscillations of a rectangular plates with two adjacent edges clamped

Собственные колебания прямоугольной пластины, защемленной по двум смежным краям

M.V. Sukhoterin*,
S.O. Baryshnikov,
T.P. Knysh,
Admiral Makarov State University of Maritime and Inland Shipping, Saint-Petersburg, Russia
R.A. Abdikarimov,
Tashkent Financial Institute, Tashkent, Uzbekistan

Д-р техн. наук, заведующий кафедрой М.В. Сухотерин*,
д-р техн. наук, ректор С.О. Барышников,
канд. физ.-мат. наук, заместитель директора института водного транспорта Т.П. Кныш,
Государственный университет морского и речного флота имени адмирала С.О. Макарова, Санкт-Петербург, Россия
д-р физ.-мат. наук, профессор Р.А. Абдикаримов,
Ташкентский финансовый институт, г. Ташкент, Узбекистан

Key words: civil and structural engineering; building and construction; rectangular plate; accurate natural frequency; resonance; fourier series

Ключевые слова: гражданское и промышленное строительство; строительные конструкции; прямоугольная плита; спектр собственных частот; резонанс; ряды Фурье

Abstract. We study the natural oscillations of a rectangular plate, two adjacent edges of which are clamped, and the other two are free (CCFF-plate), as an element of many building structures. The deflection function is chosen as a sum of two hyperbolic trigonometric series. Both series obey the main equation of free vibration. Meeting all boundary conditions of a problem leads to an infinite system of homogeneous linear algebraic equations with respect to eight series coefficients. This system is transformed in two subsystems due to four basic coefficients, for which the iterative solution process is organized. Initial values of a pair of basic coefficient series are chosen randomly. Frequency values are chosen so that iterations coincide starting with a certain number. This provides non-trivial solutions of the reduced system. For the first eight obtained natural frequencies there have been presented relevant 3D mode shapes. The paper provides accuracy analysis and its comparison with other familiar results.

Аннотация. Исследуются собственные колебания прямоугольной плиты, два смежных края которой защемлены, а два других свободны (CCFF-пластина), как элемента многих строительных конструкций. Искомая функция прогибов выбирается в виде суммы двух гиперболо-тригонометрических рядов. Оба ряда подчиняются основному уравнению собственных колебаний. Выполнение всех граничных условий задачи приводит к бесконечной системе однородных линейных алгебраических уравнений относительно восьми коэффициентов рядов. Эта система преобразуется к двум подсистемам относительно четырех базовых коэффициентов, для которых организован итерационный процесс решения. Начальные значения одной пары последовательностей базовых коэффициентов назначаются произвольно. Подбираются значения частот, при которых, начиная с некоторого номера, итерации совпадают, что дает нетривиальные решения редуцированной системы. Для найденных таким образом первых восьми собственных частот представлены соответствующие 3D формы колебаний. Приводятся анализ точности вычислений и сравнение с известными результатами.

1. Introduction

Industrial and civil buildings often have perpendicular side wings in plan. In the inner corners of buildings a rectangular balcony slab and flat roofs can be rigidly sealed to adjacent wall. The other two edges are usually free. In addition to static load, these elements can be subjected to dynamic effects. These are vibrations from various types of power units, sound or shock waves, seismic loads. The

Сухотерин М.В., Барышников С.О., Кныш Т.П., Абдикаримов Р.А. Собственные колебания прямоугольной пластины, защемленной по двум смежным краям // Инженерно-строительный журнал. 2018. № 6(82). С. 81–94.

frequencies of forced oscillations can vary in a wide range. Resonance phenomena occur not only at the first natural frequency, but also on overtones. Therefore it is important to know some initial spectrum of natural frequencies that will allow to carry out full-scale tests of the specified elements on resonance.

Application of innovative materials in construction requires improvement of computational methods to carry out high-precision calculations, in particular, dynamic ones. An accurate closed-form solution to a problem of free vibration of a rectangular CCFF plate (C – clamped edge, F – free edge) has not been provided. Usage of approximate solutions contradicts validity of the obtained numerical results. Mesh methods are often efficient, however fine mesh can lead to less accuracy due to a badly – determined matrix of the system. Such methods need testing by analytical or numerical-analytical methods.

At first the range of five natural frequencies for free vibration of a rectangular CCFF plate was obtained by Young [1] in 1950 by the Rayleigh-Ritz method using beam functions (three in each direction), which are combinations of hyperbolic and trigonometric functions. The Rayleigh-Ritz method was also used in the papers [2-7] to solve a similar problem. Leissa [2] increased a number of beam functions to 36. Dickinson and Li [3] applied double series with hyperbolic and trigonometric sine and cosine functions that satisfy the conditions of free support for opposite edges. Bhat [4] used characteristic orthogonal polynomials and the Gram-Schmidt procedure. Mizusawa [5] dealt with B-spline function. Zhang and Li [6] sought a solution in the form of the double Fourier cosine series, supplemented by several ordinary trigonometric series of a special form. The paper of Monterrubio and Ilanko [7] presents polynomials, trigonometric functions and their combinations for 55 types of boundary conditions with penalties during calculation.

In 1992 Singal et al. [8] obtained experimental data about natural frequencies of plates with different boundary conditions. This information is a reliable benchmark for theoretical calculations. In the above-mentioned paper the authors provide theoretical results that were gained using the "Analdyne-1" computer software by the Gorman method (the superposition method) [9, 10].

The papers [11–13] focus on various modifications of the Finite Element Method (FEM). Kerboua *et al.* 2007 [11] applied the semi-analytical FEM along with the Sanders Shell Theory. Patil [12] solved a problem using the Modified Discrete Kirchhoff Quadrilateral element (MDKQ) with the mesh 8×8 and 16×16. The work of Rao and Mohan [13] is based on FEM using the ANSYS software and Galerkin analytical method to determine the first frequency for different materials and boundary conditions on the crack and non-crack surfaces.

In the work [14] two-dimensional boundary value problem is reduced to one-dimensional, modifici-specific method of spline-collocation. The one-dimensional problem is solved numerically by discrete orthogonalization.

The papers [15–18] describe methods which were applied for plates with different boundary conditions. However, these papers do not contain numerical results for a CCFF plate, though they could have been used for solving this problem. Actually, the results [18] for CFFF and CCCC plates are equal to our results obtained in the papers [19–21].

In works [22–25] the questions of resonant phenomena at high frequencies are touched upon. It is noted that they are weakly expressed and are not able to cause destruction of structural elements. However, there is no analysis of the long-term impact of the disturbing force on the resonant frequencies.

One interesting recent work [26] devoted to the solution of the problem of natural vibrations in stresses, and not, as usual, in displacements.

We also note the works [27–29], devoted to the application of various computational methods for solving problems of the dynamics of structures, which can be used for this problem.

Relevance of research of own oscillations of CCFF plates is caused by their wide application in civil engineering, and also in instrument making and nanotechnologies.

The purpose of this work is to determine the initial spectrum of natural frequencies and vibration forms of a rectangular plate, two adjacent edges of which are clamped, and the other two are free. The task of the study is to build a numerical and analytical method to achieve this goal with high accuracy. The object of the study is the vibrations of the plates, and the subject of the study – the natural vibrations of the CCFF - plate.

2. Methods

2.1. Problem statement

The paper considers a rectangular Kirchhoff plate with two adjacent edges clamped ($x = 0$ and $y = 0$), and two other edges free. Let a and b be dimensions of the plate in plan, h is its thickness. It is required to find a spectrum of natural frequencies for such a plate and corresponding mode shapes.

We introduce dimensionless coordinates $x = X / b$, $y = Y / b$, hence the plate dimensions will be the following: $0 \le x \le \gamma$, $0 \le y \le 1$ where $\gamma = a / b$ (Figure 1).

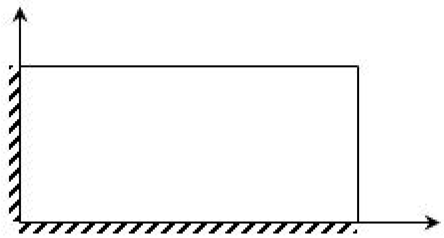

Figure 1. Rectangular CCFF plate

The differential equation of free vibrations of the plate is determined by Lekhnitskii [30]

$$\nabla^2\nabla^2 W + \eta^2 \frac{\partial^2 W}{\partial t^2} = 0\,, \tag{1}$$

where ∇^2 – is the 2D Laplace operator; $W(x, y, t)$ – is a desired function of the deflections of the middle plane of the plate; t is time, $\eta^2 = \rho h b^4 / D$, ρ is the density of the plate's material, $D = Eh^3 / \left(12(1-\nu^2)\right)$ is the cylindrical rigidity of the plate, E is Young's modulus, ν is Poisson's ratio.

According to the Fourier method, this function is written as follows:

$$W(x, y, t) = \left(C_1 \cos pt + C_2 \sin pt\right) w(x, y). \tag{2}$$

Here, C_1, C_2 are arbitrary constants, which are determined from the initial conditions; p is the unknown oscillation frequency (circular frequency) of the plate; $w(x, y)$ is a coordinate function that must satisfy the differential equation [30]:

$$\nabla^2\nabla^2 w(x, y) - \omega^2 w(x, y) = 0\,, \tag{3}$$

$\omega = p\eta = pb^2\sqrt{\rho h / D}$ – is the natural dimensionless vibration frequency. This equation is obtained by substituting (2) in (1). Function $w(x, y)$ determines mode shapes for the found frequency.

Then we will solve the problem of determining natural frequencies and mode shapes.

The desired function of the form of oscillations $w(x, y)$ is to satisfy the boundary conditions [31],

$$w = 0\,, \ \frac{\partial w}{\partial x} = 0 \ \text{at } x=0, \tag{4}$$

$$\frac{\partial^2 w}{\partial x^2} + \nu \frac{\partial^2 w}{\partial y^2} = 0, \quad \frac{\partial^3 w}{\partial x^3} + (2-\nu)\frac{\partial^3 w}{\partial x \partial y^2} = 0 \ \text{at } x = \gamma, \tag{5}$$

$$w = 0\ ,\ \frac{\partial w}{\partial y} = 0 \text{ at } y = 0, \tag{6}$$

$$\frac{\partial^2 w}{\partial y^2} + \nu\frac{\partial^2 w}{\partial x^2} = 0,\quad \frac{\partial^3 w}{\partial y^3} + (2-\nu)\frac{\partial^3 w}{\partial x^2 \partial y} = 0 \text{ at } y = 1\ , \tag{7}$$

$$\frac{\partial^2 w}{\partial x \partial y} = 0 \text{ in point } (\gamma;\ 1). \tag{8}$$

Boundary conditions show the absence of deflections and angles of rotation for clamped edges, the lack of bending moments M_x, M_y and shear forces Q_x, Q_y on free edges and the torque M_{xy} in a free angular point.

2.2. Methods

The exact solution of the problem (3–8) can be obtained if the desired deflection function is represented as the sum of two such hyperbolic-trigonometric series of sinuses of the following form

$$\begin{aligned} w(x,y) = &\sum_{k=1,3,\dots}^{\infty} [A_k \cosh\alpha_k(x-\gamma) + B_k \cosh\beta_k(x-\gamma) \\ &+ C_k \sinh\alpha_k(x-\gamma) + D_k \sinh\beta_k(x-\gamma)]\sin\lambda_k y \\ &+ \sum_{s=1,3,\dots}^{\infty} [E_s \cosh\xi_s(y-1) + F_s \cosh\eta_s(y-1) \\ &+ G_s \sinh\xi_s(y-1) + H_s \sinh\eta_s(y-1)]\sin\mu_s x \end{aligned} \tag{9}$$

where A_k, B_k, C_k, D_k, E_s, F_s, G_s, H_s are undetermined ratios,

$$\lambda_k = \frac{k\pi}{2},\quad \mu_s = \frac{s\pi}{2\gamma}. \tag{10}$$

Ratios α_k, β_k, ξ_s, η_s result from the biquadratic equations, when each series are inserted in the basic differential Equation (3):

$$\alpha_k = \sqrt{\lambda_k^2 + \omega},\ \beta_k = \sqrt{\lambda_k^2 - \omega},\quad \xi_s = \sqrt{\mu_s^2 + \omega},\quad \eta_s = \sqrt{\mu_s^2 - \omega}\ . \tag{11}$$

Note that the series (9) have only odd harmonics, which ensures symmetry in the solution due to edges $x = \gamma$ and $y = 1$. Thus, we consider the plate of $2\gamma \times 2$ dimensions with additional conditions along the symmetry axes (5, 7, 8) instead of conditions on fictitious edges $x = 2\gamma$ and $y = 2$.

It is required that the deflection function w should satisfy all boundary conditions. Primarily, deflections on the clamped edges of the plate have to go to zero (first conditions (4), (6)). This results into two equations for the unknown ratios:

$$A_k \cosh\alpha_k\gamma + B_k \cosh\beta_k\gamma - C_k \sinh\alpha_k\gamma - D_k \sinh\beta_k\gamma = 0\ , \tag{12}$$

$$E_s \cosh\xi_s + F_s \cosh\eta_s - G_s \sinh\xi_s - H_s \sinh\eta_s = 0\ . \tag{13}$$

Then the partial derivatives and their combinations included in conditions (4) – (8) are found.

The condition of the absence of rotation angles for the clamped edges (the second conditions (4), (6)) also leads to two equations:

$$\sum_{k=1,3,...}^{\infty}\left(-A_k\alpha_k\sinh\alpha_k\gamma-B_k\beta_k\sinh\beta_k\gamma+C_k\alpha_k\cosh\alpha_k\gamma+D_k\beta_k\cosh\beta_k\gamma\right)\sin\lambda_k y$$
$$+\sum_{s=1,3,...}^{\infty}\mu_s[E_s\cosh\xi_s(y-1)+F_s\cosh\eta_s(y-1)+G_s\sinh\xi_s(y-1) \qquad (14)$$
$$+H_s\sinh\eta_s(y-1)]=0.$$

$$\sum_{s=1,3,...}^{\infty}\left(-E_s\xi_s\sinh\xi_s-F_s\eta_s\sinh\eta_s+G_s\xi_s\cosh\xi_s+H_s\eta_s\cosh\eta_s\right)\sin\mu_s x$$
$$+\sum_{k=1,3,...}^{\infty}\lambda_k[A_k\cosh\alpha_k(x-\gamma)+B_k\cosh\beta_k(x-\gamma)+C_k\sinh\alpha_k(x-\gamma) \qquad (13)$$
$$+D_k\sinh\beta_k(x-\gamma)]=0\ .$$

The conditions (5) of the absence of bending moments and shear forces on the edge $x=\gamma$ provide other two equations:

$$\sum_{k=1,3,...}^{\infty}[A_k(\alpha_k^2-\nu\lambda_k^2)+B_k(\beta_k^2-\nu\lambda_k^2)]\sin\lambda_k y+\sum_{s=1,3,...}^{\infty}(-1)^{s^*+1}[E_s(-\mu_s^2+\nu\xi_s^2)\cosh\xi_s(y-1)$$
$$+F_s(-\mu_s^2+\nu\eta_s^2)\cosh\eta_s(y-1)+G_s(-\mu_s^2+\nu\xi_s^2)\sinh\xi_s(y-1) \qquad (16)$$
$$+H_s(-\mu_s^2+\nu\eta_s^2)\sinh\eta_s(y-1)]=0\,,$$
$$C_k\alpha_k[\alpha_k^2-(2-\nu)\lambda_k^2]+D_k\beta_k[\beta_k^2-(2-\nu)\lambda_k^2]=0\,, \qquad (17)$$

where $s^*=(s+1)/2$.

The conditions (7) of the absence of bending moments and shear forces on the edge $y=1$ leads to:

$$\sum_{k=1,3,...}^{\infty}(-1)^{k^*+1}[A_k(-\lambda_k^2+\nu\alpha_k^2)\cosh\alpha_k(x-\gamma)+B_k(-\lambda_k^2+\nu\beta_k^2)\cosh\beta_k(x-\gamma)$$
$$+C_k(-\lambda_k^2+\nu\alpha_k^2)\sinh\alpha_k(x-\gamma)+D_k(-\lambda_k^2+\nu\beta_k^2)\sinh\beta_k(x-\gamma)] \qquad (18)$$
$$+\sum_{s=1,3,...}^{\infty}[E_s(\xi_s^2-\nu\mu_s^2)+F_s(\eta_s^2-\nu\mu_s^2)]\sin\mu_s x=0\,,$$
$$G_s\xi_s[\xi_s^2-(2-\nu)]+H_s\eta_s[\eta_s^2-(2-\nu)]=0\,, \qquad (19)$$

where $k^*=(k+1)/2$.

Note that the condition (8) is met “automatically” by both functions (9).

In the obtained system of eight Equations (12–19) we expand hyperbolic functions in a Fourier series with the following formulae:

$$\sinh\alpha_k(x-\gamma)=-\frac{2}{\gamma}\sum_{s=1,3,...}^{\infty}\frac{(-1)^{s^*}\alpha_k+\mu_s\sinh\alpha_k\gamma}{\alpha_k^2+\mu_s^2}\sin\mu_s x,$$
$$\cosh\alpha_k(x-\gamma)=\frac{2}{\gamma}\sum_{s=1,3,...}^{\infty}\frac{\mu_s\cosh\alpha_k\gamma}{\alpha_k^2+\mu_s^2}\sin\mu_s x, \qquad (20)$$
$$\sinh\xi_s(y-1)=-2\sum_{k=1,3,...}^{\infty}\frac{(-1)^{k^*}\xi_s+\lambda_k\sinh\xi_s}{\lambda_k^2+\xi_s^2}\sin\lambda_k y,$$

$$\cosh \xi_s (y-1) = 2 \sum_{k=1,3,...}^{\infty} \frac{\lambda_k \cosh \xi_s}{\lambda_k^2 + \xi_s^2} \sin \lambda_k y \,. \tag{21}$$

Expansions $\sinh \beta_k (x-\gamma)$, $\cosh \beta_k (x-\gamma)$, $\sinh \eta_s (y-1)$, $\cosh \eta_s (y-1)$ result from the above-mentioned by substituting α_k for β_k and ξ_s for η_s.

The formulae (17) and (19) lead to

$$D_k = -\frac{\alpha_k}{\beta_k} \varphi_k C_k, \quad H_s = -\frac{\xi_s}{\eta_s} \psi_s G_s \;. \tag{22}$$

where

$$\varphi_k = \frac{(1-\nu)\lambda_k^2 - \omega}{(1-\nu)\lambda_k^2 + \omega}, \; \psi_s = \frac{(1-\nu)\mu_s^2 - \omega}{(1-\nu)\mu_s^2 + \omega}. \tag{23}$$

Insert (22) into (12) and (13), then solve the equations due to C_k and G_s

$$C_k = \frac{A_k^* + B_k^*}{\delta_k \sinh \alpha_k \gamma}, \; G_s = \frac{E_s^* + F_s^*}{\tau_s \sinh \xi_s}, \tag{24}$$

Where

$$A_k^* = A_k \cosh \alpha_k \gamma \,, \; B_k^* = B_k \cosh \beta_k \gamma \,, \; E_s^* = E_s \cosh \xi_s \;, \; F_s^* = F_s \cosh \eta_s$$

$$\delta_k = 1 - \frac{\alpha_k}{\beta_k} \varphi_k \frac{\sinh \beta_k \gamma}{\sinh \alpha_k \gamma}, \; \tau_s = 1 - \frac{\xi_s}{\eta_s} \psi_s \frac{\sinh \eta_s}{\sinh \xi_s}. \tag{25}$$

Now substitute (22), (24), and expansions (20), (21) in (14) and (15), change the order of summation in double series, disable the external summation. Then obtain the equations:

$$a_{11} A_k^* + a_{12} B_k^* = b_1 \,, \; \tilde{a}_{11} E_s^* + \tilde{a}_{12} F_s^* = \tilde{b}_1 \,, \tag{26}$$

where

$$a_{11} = \alpha_k \left[\frac{\coth \alpha_k \gamma}{\delta_k} \left(1 - \varphi_k \frac{\cosh \beta_k \gamma}{\cosh \alpha_k \gamma} \right) - \tanh \alpha_k \gamma \right],$$

$$a_{12} = \beta_k \left[\frac{\alpha_k}{\beta_k} \frac{\coth \alpha_k \gamma}{\delta_k} \left(1 - \varphi_k \frac{\cosh \beta_k \gamma}{\cosh \alpha_k \gamma} \right) - \tanh \alpha_k \gamma \right],$$

$$b_1 = -2 \sum_{s=1,3,...}^{\infty} \mu_s \left[E_s^* \left(\frac{\lambda_k}{\lambda_k^2 + \mu_s^2 + \omega} - \varepsilon_{sk} \right) + F_s^* \left(\frac{\lambda_k}{\lambda_k^2 + \mu_s^2 - \omega} - \varepsilon_{sk} \right) \right],$$

$$\tilde{a}_{11} = \xi_s \left[\frac{\coth \xi_s}{\tau_s} \left(1 - \psi_s \frac{\cosh \eta_s}{\cosh \xi_s} \right) - \tanh \xi_s \right],$$

$$\tilde{a}_{12} = \eta_s \left[\frac{\xi_s}{\eta_s} \frac{\coth \xi_s}{\tau_s} \left(1 - \psi_s \frac{\cosh \eta_s}{\cosh \xi_s} \right) - \tanh \xi_s \right].$$

$$\tilde{b}_1 = -\frac{2}{\gamma} \sum_{k=1,3,...}^{\infty} \lambda_k \left[A_k^* \left(\frac{\mu_s}{\lambda_k^2 + \mu_s^2 + \omega} - \chi_{ks} \right) + B_k^* \left(\frac{\mu_s}{\lambda_k^2 + \mu_s^2 - \omega} - \chi_{ks} \right) \right]. \tag{27}$$

Here

$$\varepsilon_{sk}=\frac{1}{\tau_s\sinh\xi_s}\left(\frac{(-1)^{k^*}\xi_s+\lambda_k\sinh\xi_s}{\lambda_k^2+\mu_s^2+\omega}-\frac{\xi_s}{\eta_s}\psi_s\frac{(-1)^{k^*}\eta_s+\lambda_k\sinh\eta_s}{\lambda_k^2+\mu_s^2-\omega}\right),$$

$$\chi_{ks}=\frac{1}{\delta_k\sinh\alpha_k\gamma}\left(\frac{(-1)^{s^*}\alpha_k+\mu_s\sinh\alpha_k\gamma}{\lambda_k^2+\mu_s^2+\omega}-\frac{\alpha_k}{\beta_k}\varphi_k\frac{(-1)^{s^*}\beta_k+\mu_s\sinh\beta_k\gamma}{\lambda_k^2+\mu_s^2-\omega}\right).$$

Now substitute (22), (24), and expansions (20), (21) in (16) and (18), change the order of summation in double series, disable the external summation. Then obtain the equations:

$$a_{21}A_k^*+a_{22}B_k^*=b_2\,,\ \tilde{a}_{21}E_s^*+\tilde{a}_{22}F_s^*=\tilde{b}_2\ , \tag{28}$$

where

$$a_{21}=\frac{(1-\nu)\lambda_k^2+\omega}{\cosh\alpha_k\gamma},\quad a_{22}=\frac{(1-\nu)\lambda_k^2-\omega}{\cosh\beta_k\gamma},$$

$$b_2=2\sum_{s=1,3,...}^{\infty}(-1)^{s^*+1}\left[E_s^*\left(\frac{\lambda_k\left[(1-\nu)\mu_s^2-\nu\omega\right]}{\lambda_k^2+\mu_s^2+\omega}-\tilde{\varepsilon}_{sk}\right)\right.$$

$$\left.+F_s^*\left(\frac{\lambda_k\left[(1-\nu)\mu_s^2+\nu\omega\right]}{\lambda_k^2+\mu_s^2-\omega}-\tilde{\varepsilon}_{sk}\right)\right],$$

$$\tilde{a}_{21}=\frac{(1-\nu)\mu_s^2+\omega}{\cosh\xi_s},\quad \tilde{a}_{22}=\frac{(1-\nu)\mu_s^2-\omega}{\cosh\eta_s}, \tag{29}$$

$$\tilde{b}_2=\frac{2}{\gamma}\sum_{k=1,3,...}^{\infty}(-1)^{k^*+1}\left[A_k^*\left(\frac{\mu_s\left[(1-\nu)\lambda_k^2-\nu\omega\right]}{\lambda_k^2+\mu_s^2+\omega}-\chi_{ks}\right)\right.$$

$$\left.+B_k^*\left(\frac{\mu_s\left[(1-\nu)\lambda_k^2+\nu\omega\right]}{\lambda_k^2+\mu_s^2-\omega}-\chi_{ks}\right)\right].$$

Here

$$\tilde{\varepsilon}_{sk}=\frac{1}{\tau_s\sinh\xi_s}\left(\frac{(-1)^{k^*}\xi_s+\lambda_k\sinh\xi_s}{\lambda_k^2+\mu_s^2+\omega}\left[(1-\nu)\mu_s^2-\nu\omega\right]\right.$$

$$\left.-\frac{\xi_s}{\eta_s}\psi_s\frac{(-1)^{k^*}\eta_s+\lambda_k\sinh\eta_s}{\lambda_k^2+\mu_s^2-\omega}\left[(1-\nu)\mu_s^2+\nu\omega\right]\right),$$

$$\tilde{\chi}_{ks}=\frac{1}{\delta_k\sinh\alpha_k\gamma}\left(\frac{(-1)^{s^*}\alpha_k+\mu_s\sinh\alpha_k\gamma}{\lambda_k^2+\mu_s^2+\omega}\left[(1-\nu)\lambda_k^2-\nu\omega\right]\right.$$

$$\left.-\frac{\alpha_k}{\beta_k}\varphi_k\frac{(-1)^{s^*}\beta_k+\mu_s\sinh\beta_k\gamma}{\lambda_k^2+\mu_s^2-\omega}\left[(1-\nu)\lambda_k^2+\nu\omega\right]\right).$$

Now the Equations (26), (28) are combined into two symmetric homogeneous systems, from which it is required to find values ω to provide non-trivial solutions

$$\begin{cases} a_{11}A_k^* + a_{12}B_k^* = b_1 = b_1(E_s^*, F_s^*) \\ a_{21}A_k^* + a_{22}B_k^* = b_2 = b_2(E_s^*, F_s^*) \end{cases}, \quad (30)$$

$$\begin{cases} \tilde{a}_{11}E_s^* + \tilde{a}_{12}F_s^* = \tilde{b}_1 = \tilde{b}_1(A_k^*, B_k^*) \\ \tilde{a}_{21}E_s^* + \tilde{a}_{22}F_s^* = \tilde{b}_2 = \tilde{b}_2(A_k^*, B_k^*) \end{cases}. \quad (31)$$

The right-handed parts of the system (30) have ratios E^*_s, F^*_s in the sigma notation, which are found from solving the system (31). Besides, in its right-handed parts under the summation sign the system (31) has ratios A^*_k, B^*_k, which can be regarded as ratios of the previous iteration. The ratios for the initial iteration, for example, can be fixed as equal to one. Ratios E^*_s, F^*_s, which resulted from the system (31), are substituted in the system (30) to obtain ratios A^*_k, B^*_k of a new iteration. Hereby the iterative process of finding ratios A^*_k, B^*_k, E^*_s, F^*_s is organized.

Both systems as a parameter contain vibration frequency ω, which should be set. Changing the frequency, it is possible to pick up its value in such a way that corresponding ratios for all subsequent iterations, starting from a certain one, will be similar (and non-trivial). This frequency is the required natural frequency, with which the systems (30), (31) will have non-trivial solutions. It is in line with mode shapes of the free vibration which can be obtained in a 3D format, using the formulae (9). This method was effectively used in the papers [19–21] for a cantilever or clamped plate.

3. Results and Discussion

The spectrum of natural frequencies was determined using software product Maple in the course of the iterative process of finding non-trivial solutions to the reduced homogeneous system of linear algebraic equations. The following parameters were variable: the frequency of vibrations, the ratio of sides of the plate, the number of terms held in the series (the size of the reduced system), the number of iterations, the number of significant digits in calculations, the number of digits displayed on the screen as a result of calculations, the initial values of the ratios A^*_{k0}, B^*_{k0}. The following basic ratios A^*_k, B^*_k, E^*_s, F^*_s were displayed at each iteration, which allowed us to control the iterative process. The standard values of the number of iterations were m = 20, 25, i.e. it was assumed to be sufficient to conclude about the iterations convergence or divergence at the chosen frequency when the ratios of the neighboring iterations were compared. If the ratios, while decreasing in absolute value, tended to zero or increased indefinitely, a new frequency value was assigned. The number of terms in the series was chosen to be equal to n = 29, 39, 49, 59, 69 to clarify the results in the neighborhood of the desired natural frequency. If the process turned out to be poorly converging in the area of separate frequencies, the number of iterations was increased up to 50, 100, 200, ..., 1000 and more.

We considered a square plate as a numerical example. Note that the values obtained by other authors served as a reference to select intervals to search for the first six natural frequencies. The criterion for the closeness of the frequency to the natural one was a slow change in the ratios, beginning from a certain iteration. The frequency at which the neighboring iterations began to coincide up to 4-5 signs was taken as a natural frequency. The search for natural frequencies whose mode shapes were symmetric with respect to the main diagonal did not take much time.

It was much more difficult to search for the natural frequencies of antisymmetric mode shapes. Due to a slow convergence of the process in the neighborhood of the desired natural frequency, it was necessary to increase greatly the number of iterations. The antisymmetric frequencies ω_2 and ω_7 take a special position here. When searching for ω_2 it was found from the behavior of the ratios that in the neighborhood of value ω = 23.49015 (n = 49), the ratios with growing iterations (we investigated the range up to 9000 iterations. The computing time is about 30 minutes) changed roughly in accordance with the Law of Harmony $A(m)\sin(m/2)$ with a variable amplitude. Moreover, the amplitude slowly decreased down to the specified value and then increased. At a value of 23.49015, amplitude A remained constant, the sequence became almost strictly periodic, i.e. it did not tend to any limit. Comparison of the 3D mode shapes at adjacent iterations showed that for amplitude values of the ratios the mode shape was close to the expected one (with a nodal line at the main diagonal). The maximum deviation from the straight line was approximately 3.5 % with respect to the maximum amplitude of the mode shape. Then the mode was distorted and after six iterations acquired the same shape again, but of the opposite direction. This phenomenon was unexpected. Perhaps the paradox is due to the instability of the very shape of antisymmetric vibrations, its "blurring". A negative result was achieved in thorough search for any other value in the frequency range 23 ≤ ω ≤ 25, which could be the natural frequency. The study made it possible to take the approximate value ~ 23.49 as the second natural (unstable) frequency ω_2.

Search for the next antisymmetric natural frequency ω_5 was standard, in contrast to ω_2. The frequency ω_5 = 62.7025 and the corresponding mode shape could be found for n = 49 after 1000 iterations. There was a coincidence of the values of the neighboring iterations by three significant digits (the difference in the fourth one is not more than one). When n = 59 we obtained ω_5 = 62.7038 after 2500 iterations, with an error in the fourth digit not more than one.

Like the first frequency ω_7, the third antisymmetric frequency ω_7 = 82.2325 was found roughly after numerous calculations with a wide variation in the number of terms in the series, the number of iterations, the initial values of the base ratios. With a growth in iterations the ratios changed around this value roughly in accordance with the harmonic law $A(m)\sin(m)$ with a variable amplitude: on the left it was decreasing, on the right it was increasing. At a value of 82.2325, the amplitude became constant. The corresponding mode shape was also unstable. The best mode shape had the greatest deviation from the main diagonal of about 10 % with respect to the maximum amplitude of the mode shape.

The numerical results obtained in this work are given in the upper rows of Table 1.The corresponding mode forms of natural vibrations are shown in Figures 2–9. The following rows of the table show the theoretical results of other authors, as well as the experimental data of Singal *et al.* [8].

Table 1. Comparison of the dimensionless natural frequencies of the square CCFF plate ($\omega = pb^2\sqrt{\rho h / D}$) for ν = 0.3

Theory	Natural frequencies							
	ω_1	ω_2	ω_3	ω_4	ω_5	ω_6	ω_7	ω_8
	S	A	S	S	A	S	A	S
Present theory	m=20	–	m=50	m=25	m=2500	m=25	–	m=300
n=69	6.9189	–	26.5845	47.6487	62.7038*	65.5293	–	88.34705
	m=20	m=3000	m=25	m=25	m=1000	m=25	m=3000	m=80
n=49	6.9188	23.49	26.5843	47.6505	62.7025	65.5298	82.2325	88.3448
Young [1]	6.958	24.08	26.80	48.05	63.14	–	–	–
Leissa[2]	6.9421	24.034	26.681	47.785	63.039	65.833	–	–
Dickinson[3]	7.1631	23.974	26.687	47.753	62.967	65.772	–	–
Bhat[4]	6.9243	23.923	26.591	47.670	62.850	65.685	–	–
Mizusawa[5]	6.883	23.70	26.56	47.34	62.54	–	–	–
Kerboua[11]	6.92	23.96	26.50	47.23	62.77	65.65	–	–
Patil[12]	7.007	24.208	–	–	–	–	–	–
Monterrubio[7]	6.92	23.905	26.585	47.653	62.708	65.535	–	–
Singal[8]	6.86	23.59	26.53	47.20	62.26	65.46	–	–
Experiment							–	–
Singal[8]	6.85	23.61	26.58	48.33	63.08	65.75	–	–

S is a symmetric mode shape, A is an antisymmetric mode shape (with respect to the diagonal); the value 62.7038* is obtained for n = 59.

Note that Mizusawa [5] has confused data for the CFCF and FFCC plates. To match the formula $\omega = pb^2\sqrt{\rho h / D}$, the data obtained by Singal *et al.* [8] divided by a conversion factor of 6.06, and the data presented by Patil [12] is multiplied by 10.

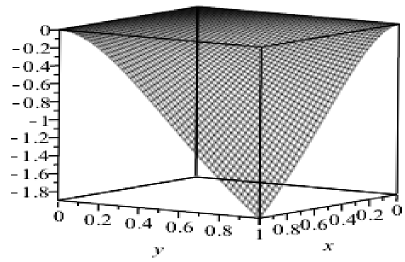

Figure 2. The first mode shape at frequency ω_1 = 6.9189

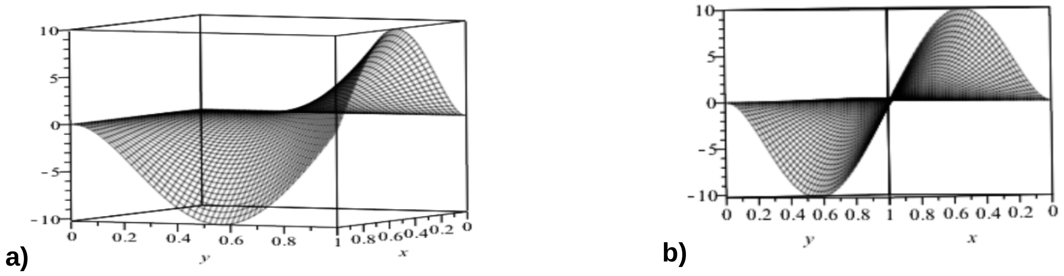

Figure 3. The second mode shape at frequency ω_2 = 23.49: (a) 3D shape, (b) view from the diagonal

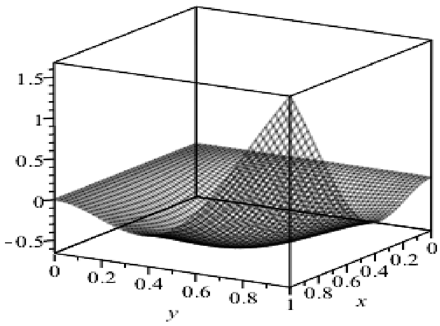

Figure 4. The third mode shape at frequency ω_3 = 26.5843

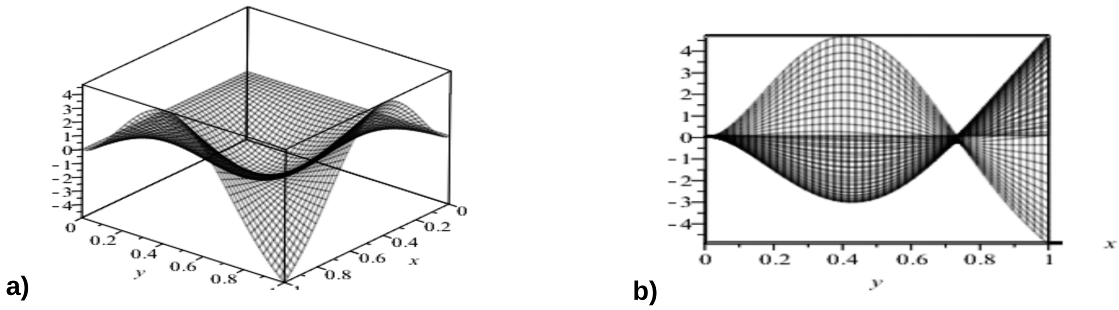

Figure 5. The fourth mode shape at frequency ω_4 = 47.6505: (a) 3D shape, (b) view from the Ox axis

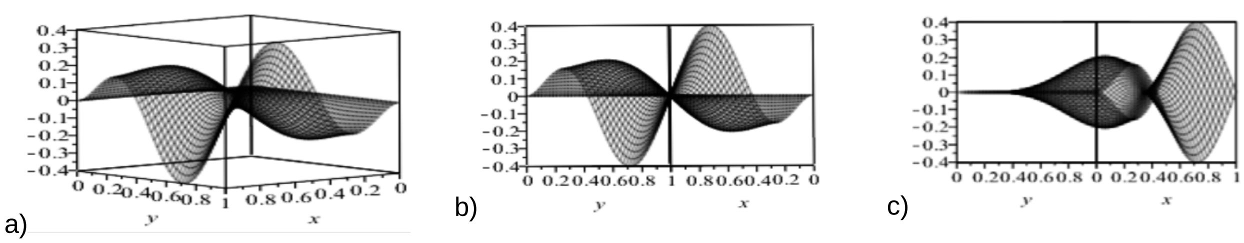

Figure 6. The fifth mode shape at frequency ω_5 = 62.7025: (a) 3D shape, (b) view from the main diagonal, (c) view from the other diagonal

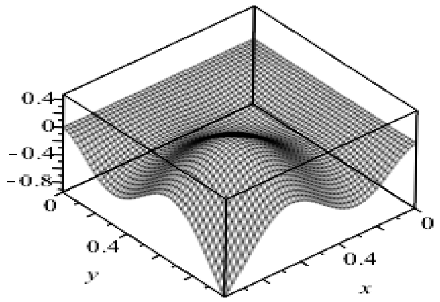

Figure 7. The sixth mode shape at frequency ω_6 = 65.5298

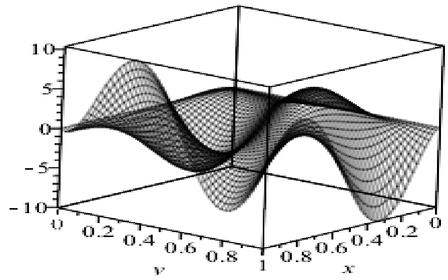

Figure 8. The seventh mode shape at frequency ω_7 = 82.2325

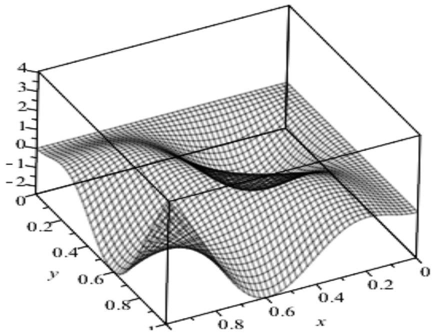

Figure 9. The eighth mode shape at frequency ω_8 = 88.34705

The frequencies of the natural vibrations calculated in this work are in good agreement with the experimental data obtained in the work by Singal *et al.* [8]. Comparison with the theoretical results correspond well to the data by [8], Bhat [4], Kerboua *et al.* [11], Monterrubio and Ilanko [7], which has been obtained with accurate calculations.

It should be noted here that it is difficult to provide a clamped edge in the experiment, so the experimental frequencies for the CCFF plate [8] should be slightly lower than the corresponding sufficiently accurate analytical frequencies. However, the authors [8] have reversed results, starting from the second frequency. In our solution, the "correct" pattern is manifested for the first and third frequency, which is then violated for higher frequencies, too. Such an effect can be explained by the influence of inertial forces and deformation of the transverse shear at high frequencies, which are not considered in the theoretical Kirchhoff model. Comparison with Young's results [1] bears such evidence too.

Romakina [14] calculated the first three resonant frequencies and obtained the corresponding symmetric 3D forms of plate oscillations from different materials in the presence of transverse sinusoidal load. These forms are similar to those obtained in this paper.

The fact that the values of the second (antisymmetric) frequency differ significantly in the works by different authors: from 23.59 to 24.08 indicates the instability of calculations at this frequency. We note that the approximate value of 23.49 obtained in this work (the least value listed in the table) is the closest to the values (experimental and theoretical) obtained in the work [8].

Note also that in the works [1–5, 7, 8, 11, 12] 3D forms of natural oscillations have not been obtained.

4. A note on the initial condition problem

If a certain spectrum of n natural frequencies and vibration forms is found, then the nearest solution of the problem, according to (2), is written as follows:

$$W(x,y,t)=\sum_{i=1}^{N}\left(C_{1i}\cos p_i t+C_{2i}\sin p_i t\right)w_i(x,y)$$

where i = 1, 2,..., N the order number of the eigenfrequencies found (in general, there should be an infinite set);

$$w_i = w_{1i} + w_{2i}.$$

The problem can be solved to the end if the initial conditions are given:

$$W(x,y,t)|_{t=0}=W_0(x,y), \quad \frac{\partial W}{\partial t}|_{t=0}=V_0(x,y)$$

where $W_0(x, y)$ and $V_0\ (x, y)$ are the initial deflections and velocities of the plate points.

Setting initial conditions is a separate complex task. The field of initial displacements of the plate points $W_0(x, y)$ and the field of initial velocities $V_0\ (x, y)$ should correspond to the real physical state of the plate at the initial time. Often, free oscillations begin after the static transverse load is momentarily terminated. Then it is necessary to solve the problem of bending such a plate, and the found function of deflections will be the field of initial displacements. The initial velocity field will be zero. More complex are the cases of application of shock load, etc.

If the initial conditions are set, the coefficients in the expression (2) will be found from the system of equations

$$\begin{cases} \sum_{i}^{N} C_{1i} w_i(x,y) = W_0(x,y), \\ \sum_{i}^{N} C_{2i} p_i w_i(x,y) = V_0(x,y). \end{cases}$$

This will in turn require the decomposition of the functions on the right side of the equalities into rows by the w_i own functions, which is also a separate challenge.

5. Conclusions

1. In this paper we propose an efficient algorithm for finding eigenfrequencies and vibration forms of CCFF-plates.

2. The spectrum of eight eigenfrequencies for a square plate and corresponding 3D waveforms are obtained with high accuracy.

3. Two special antisymmetric forms of oscillations from the mentioned spec-tra are revealed, for which the computational process is unstable.

4. The obtained numerical results are shown to be in good agreement with the results of other authors who used other high-precision methods.

6. Acknowledgement

The authors express their gratitude to the government for the financial support of this research.

The authors would like to gratefully acknowledge the unknown reviewers for their review and helpful comments.

References

1. Young, D. Vibration of rectangular plates by the Ritz method. Journal of Applied Mechanics. 1950. No. 4(17). Pp. 448–453.
2. Leissa, A.W. The free vibration of rectangular plates. Journal of Sound and Vibration. 1973. No. 3(31). Pp. 257–293.
3. Dickinson, S.M., Li, E.K.H. On the use of simply-supported plate functions in the Rayleigh-Ritz method applied to the flexural vibration of rectangular plates. Journal of Sound and Vibration. 1982. No. 2(80). Pp. 292–297.
4. Bhat, R.B. Natural frequencies of rectangular plates using characteristic orthogonal polynomials in Rayleigh-Ritz method. Journal of Sound and Vibration. 1985. No. 4(102). Pp. 493–499.
5. Mizusawa, T. Natural frequencies of rectangular plates with free edges. Journal of Sound and Vibration. 1986. No. 3(105). Pp. 451–459.
6. Zhang, X., Li, W.L. A unified approach for predicting sound radiation from baffled rectangular plates with arbitrary

Литература

1. Young D. Vibration of rectangular plates by the Ritz method // Journal of Applied Mechanics. 1950. No. 4(17). Pp. 448–453.
2. Leissa A.W. The free vibration of rectangular plates // Journal of Sound and Vibration. 1973. No. 3(31). Pp. 257–293.
3. Dickinson S.M., Li E.K.H. On the use of simply–supported plate functions in the Rayleigh-Ritz method applied to the flexural vibration of rectangular plates // Journal of Sound and Vibration. 1982. No. 2(80). Pp. 292–297.
4. Bhat R.B. Natural frequencies of rectangular plates using characteristic orthogonal polynomials in Rayleigh-Ritz method // Journal of Sound and Vibration. 1985. No. 4(102). Pp. 493–499.
5. Mizusawa T. Natural frequencies of rectangular plates with free edges // Journal of Sound and Vibration. 1986. No. 3(105). Pp. 451–459.

boundary conditions. Journal of Sound and Vibration. 2010. No. 25(329). Pp. 5307–5320.

7. Monterrubio, L.E., Ilanko, S. Proof of convergence for a set of admissible functions for the Rayleigh-Ritz analysis of beams and plates and shells of rectangular plan form. Computers and Structures. 2015. Vol. 147. Pp. 236–243.
8. Singal, R.K., Gorman, D.J., Forgues, S.A. A comprehensive analytical solution for free vibration of rectangular plates with classical edge conditions: experimental verification. Experimental Mechanics. 1992. No. 1(32). Pp. 21–23.
9. Gorman, D.J. Free Vibration Analysis of Rectangular Plates. Elsevier, Amsterdam. 1982. 324 p.
10. Gorman, D.J., Yu, S.D. A review of the superposition method for computing free vibration eigenvalues of elastic structures. Computers and Structures. 2012. Vol. 104–105. Pp. 27–37.
11. Kerboua, Y., Lakis, A.A., Thomas, M., Marcouiller, L. Hybrid method for vibration analysis of rectangular plates. Nuclear Engineering and Desing. 2007. No. 237. Pp. 791–801.
12. Patil, A.S. Free vibration analysis of thin isotropic rectangular plate. International Journal of Innovative Research in Science, Engineering and Technology. 2014. No. 4(3). Pp. 77–80.
13. Rao, P. S., Mohan, D. M. Theoretical and numerical modal analysis of aluminum and glass fiber reinforced polymer composite cracked plate. International Journal of Mechanical Engineering. 2017. No. 5 (Special Issue). Pp. 16–25.
14. Romakina, O.M. Ob ustanovivshikhsya poperechnykh kolebaniyakh pryamougolnoy plastiny iz ortotropnogo materiala [On the steady transverse vibrations of a rectangular plate made of orthotropic material]. Izvestiya Saratovskogo universiteta. Novaya seriya. Seriya Matematika. Mekhanika. Informatika. 2010. Vol. 10. No. 1. Pp. 71–77. (rus)
15. Zhu, Q., Wang, X. Free vibration analysis of thin isotropic and anisotropic rectangular plates by the discrete singular convolution algorithm. International Journal for Numerical Methods in Engineering. 2011. No. 6(86). Pp. 782–800.
16. Xing, Y.F., Xu, T.F., Solution methods of exact solutions for free vibration of rectangular orthotropic thin plates with classical boundary conditions. Composite Structures. 2013. No. 10(104). Pp. 187–195.
17. Papkov, S.O., Banerjee, J.R. A new method for free vibration and buckling analysis of rectangular orthotropic plates. Journal of Sound and Vibration. 2015. No. 3(339). Pp. 342–358.
18. Liu, X., Banerjee, J.R. Free vibration analysis for plates with arbitrary boundary conditions using a novel spectral-dynamic stiffness method. Computers and Structures. 2016. No. 11(164). Pp. 108–126.
19. Sukhoterin, M.V. Sobstvennyye kolebaniya pryamou–golnoy konsolnoy plastiny [The natural oscillation of rectangular cantilever plate]. Structural Mechanics and Analysis of Constructions. 2014. No. 2. Pp. 24–26.
20. Sukhoterin, M.V., Baryshnikov, S.O., Aksenov, D.A. Free vibration analysis of rectangular cantilever plates using the hyperbolic–trigonometric series. American Journal of Applied Sciences. 2016. No. 12(13). Pp. 1442–1451.
21. Sukhoterin, M.V., Baryshnikov, S.O., Aksenov, D.A. Sobstvennyye kolebaniya tonkikh pryamougolnykh elementov sudovykh konstruktsiy [Natural vibrations of thin rectangular elements of ship structures]. Vestnik gosudarstvennogo universiteta morskogo i rechnogo flota imeni admirala S.O. Makarova. 2016. No. 4(38). Pp. 105–113.
22. Abdikarimov, R.A., Eshmatov, Kh., Bobanazarov, Sh.P., Hodzhayev, D.A., Eshmatov, B.Kh. Mathematical modelling and calculation of hydraulic engineering constructions such as dam-plate in view of hydrodynamical pressure of water

6. Zhang X., Li W.L. A unified approach for predicting sound radiation from baffled rectangular plates with arbitrary boundary conditions // Journal of Sound and Vibration. 2010. No. 25(329). Pp. 5307–5320.
7. Monterrubio L.E., Ilanko S. Proof of convergence for a set of admissible functions for the Rayleigh-Ritz analysis of beams and plates and shells of rectangular plan form // Computers and Structures. 2015. Vol. 147. Pp. 236–243.
8. Singal R.K., Gorman D.J., Forgues S.A. A comprehensive analytical solution for free vibration of rectangular plates with classical edge conditions: experimental verification // Experimental Mechanics. 1992. No. 1(32). Pp. 21–23.
9. Gorman D.J. Free Vibration Analysis of Rectangular Plates. Elsevier, Amsterdam. 1982. 324 p.
10. Gorman D.J., Yu S.D. A review of the superposition method for computing free vibration eigenvalues of elastic structures // Computers and Structures. 2012. Vol. 104-105. Pp. 27–37.
11. Kerboua Y., Lakis A.A., Thomas M., Marcouiller L. Hybrid method for vibration analysis of rectangular plates // Nuclear Engineering and Desing. 2007. No. 237. Pp. 791–801.
12. Patil A.S. Free vibration analysis of thin isotropic rec–tangular plate // International Journal of Innovative Research in Science, Engineering and Technology. 2014. No. 4(3). Pp. 77–80.
13. Rao P. S., Mohan D. M. Theoretical and numerical modal analysis of aluminum and glass fiber reinforced polymer composite cracked plate // International Journal of Mechanical Engineering. 2017. No. 5 (Special Issue). Pp. 16–25.
14. Ромакина О.М. Об установившихся поперечных колебаниях прямоугольной пластины из ортотроп–ного материала // Известия Саратовского университе–та. Новая серия. Серия Математика. Механика. Информатика. 2010. т.10. вып.1. С. 71–77.
15. Zhu Q., Wang X. Free vibration analysis of thin iso–tropic and anisotropic rectangular plates by the discrete singular convolution algorithm // International Journal for Numerical Methods in Engineering. 2011. No. 6(86). Pp. 782–800
16. Xing Y.F., Xu T.F., Solution methods of exact solutions for free vibration of rectangular orthotropic thin plates with classical boundary conditions // Composite Structures. 2013. No. 10(104). Pp. 187–195.
17. Papkov S.O., Banerjee J.R. A new method for free vibration and buckling analysis of rectangular orthotropic plates // Journal of Sound and Vibration. 2015. No. 3(339). Pp. 342–358.
18. Liu X., Banerjee J.R. Free vibration analysis for plates with arbitrary boundary conditions using a novel spectral–dynamic stiffness method // Computers and Structures. 2016. No. 11(164). Pp. 108– 126.
19. Сухотерин М.В. Собственные колебания прямоугольной консольной пластины // Строительная механика и расчет сооружений. 2014. № 2. С. 24–26.
20. Sukhoterin M.V., Baryshnikov S.O., Aksenov D.A. Free vibration analysis of rectangular cantilever plates using the hyperbolic–trigonometric series // American Journal of Applied Sciences. 2016. No. 12(13). Pp. 1442–1451.
21. Сухотерин М.В., Барышников С.О., Аксенов Д.А. Собственные колебания тонких прямоугольных элементов судовых конструкций // Вестник государственного университета морского и речного флота им. адмирала С.О. Макарова. 2016. № 4(38). С. 105–113.

and seismic loading. Magazine of Civil Engineering. 2011. No. 3. Pp. 59–70. (rus)

23. Kozinets, G.L. Determination the dynamic performance of structures contacting with water, on the example of the arch concrete dam of Sayano-Shushenskaya HPP. Magazine of Civil Engineering. 2011. No. 5. Pp. 43–48. (rus)
24. Denisov, G.V., Lalin, V.V. About the continuous spectrum of vibrations of beam construction elements under high-frequency effects. Magazine of Civil Engineering. 2012. № 1(27). Pp. 91–97. (rus)
25. Tyukalov, Yu.Ya. Stress finite element models for determining the frequencies of free oscillations. Magazine of Civil Engineering. 2016. No. 7. Pp. 39–54. doi: 10.5862/MCE.67.5
26. Sergeyev, O.A., Kiselev, V.G., Sergeyeva, S.A. Optimal design of 3d frame structures taking into account the stress and multiple natural frequency constraints. Magazine of Civil Engineering. 2016. No. 1. Pp. 74–81. (rus) doi: 10.5862/MCE.61.7
27. Lukashevich, A., Rozin, L. Numerical decision of problems of structural mechanics with nonideal unilateral constraints. Applied Mechanics and Materials. 2014. Vols. 580–583. Pp. 2932–2935.
28. Lalin, V.V., Rybakov, V.A., Morozov, S.A. The Finite Elements Research for Calculation of Thin-Walled Bar Systems. Magazine of Civil Engineering. 2012. № 1(27). Pp. 53–73. (rus)
29. Dyakov, S.F., Lalin, V.V. Dispersiya krutilnoy volny, rasprostranyayushchayasya v tonkostennom sterzhne [Torsional wave dispersion propagating in a thin–walled rod]. Internet– zhurnal Naukovedeniye. 2013. No. 5(18). P. 24.
30. Lekhnitskii, S.G. Anisotropic Plates. Gordon&Breach Science Publishers, 1968. 534 p.
31. Timoshenko, S., Woinowsky–Krieger, S. Theory of Plates and Shells. McGraw–Hill Book Company, Inc.– New York, Toronto, London, 1959. 595 p.

22. Абдикаримов Р.А., Эшматов Х., Бобаназаров Ш.П., Ходжаев Д.А., Эшматов Б.Х. Математическое модели–рование и расчет гидротехнических сооружений типа плотины–пластины с учетом сейсмической нагрузки и гидродинамического давления воды // Инженерно-строительный журнал. 2011. № 3. С. 59–70.
23. Козинец Г.Л. Определение динамических характеристик сооружений, контактирующих с водой, на примере арочной бетонной плотины Саяно–Шушенской ГЭС // Инженерно-строительный журнал. 2011. № 5. С. 43–48.
24. Денисов Г.В., Лалин В.В. О сплошном спектре колебаний балочных элементов конструкции при высокочастотных воздействиях // Инженерно-строительный журнал. 2012. № 1(27). С. 91–97.
25. Тюкалов Ю.Я. Определение частот свободных колебаний методом конечных элементов в напряжениях // Инженерно–строительный журнал. 2016. № 7(67). С. 39–54.
26. Сергеев О.А., Киселев В.Г., Сергеева С.А. Оптимальное проектирование рам с учетом ограничений по прочности и кратным частотам собственных колебаний // Инженерно–строительный журнал. 2016. № 1(61). С. 74–81.
27. Lukashevich A., Rozin L. Numerical decision of problems of structural mechanics with nonideal unilateral constraints // Applied Mechanics and Materials. 2014. Vols. 580–583. Pp. 2932–2935.
28. Лалин В.В., Рыбаков В.А., Морозов С.А. Исследование конечных элементов для расчета тонкостенных стержневых систем // Инженерно-строительный журнал. 2012. №1(27). С. 53–73.
29. Дьяков С.Ф., Лалин В.В. Дисперсия крутильной волны, распространяющаяся в тонкостенном стержне // Интернет-журнал Науковедение. 2013. № 5(18). С. 24.
30. Lekhnitskii S.G. Anisotropic Plates. Gordon&Breach Science Publishers, 1968. 534 p.
31. Timoshenko S., Woinowsky-Krieger S., Theory of Plates and Shells, McGraw-Hill Book Company, Inc.- New York, Toronto, London, 1959. 595 p.

Mikhail Sukhoterin,*
+7(921)579-25-35; mv@sukhoterin.com

Sergey Baryshnikov,
+7(812)251-12-21; rector@gumrf.ru

Tatiana Knysh,
+7(812)748-96-73; KnyshTP@gumrf.ru

Rustamkhan Abdikarimov,
+7(99890)928-45-54; rabdikarimov@mail.ru

Михаил Васильевич Сухотерин,*
+7(921)579-25-35;
эл. почта: mv@sukhoterin.com

Сергей Олегович Барышников,
+7(812)251-12-21; эл. почта: rector@gumrf.ru

Татьяна Петровна Кныш,
+7(812)748-96-73;
эл. почта: KnyshTP@gumrf.ru

Рустамхан Алимханович Абдикаримов,
+7(99890)928-45-54;
эл. почта: rabdikarimov@mail.ru